Precision Separated-Oscillatory-Field Measurement of the $n = 10$ $^+F_3$-$^+G_4$ Interval in Helium: A Precision Test of Long-Range Relativistic, Radiative, and Retardation Effects

C. H. Storry, N. E. Rothery, and E. A. Hessels

Department of Physics, York University, 4700 Keele Street, Toronto, Ontario, Canada M3J 1P3

(Received 17 May 1995; revised manuscript received 16 August 1995)

We have measured the $^+F_3$-$^+G_4$ interval in $n = 10$ of helium to be 2017.3258(4) MHz (an accuracy of 200 ppb). The measurement uses a fast neutral beam and Ramsey separated-oscillatory-field microwave-induced transitions. When compared to recent high-precision variational calculations, it provides a high-precision test of physics (including relativistic, radiative, and retardation effects) on the large distance scale of these Rydberg atoms. The comparison indicates either that the expected long-range Casimir effect is not present, or the presence of new long-range physics.

PACS numbers: 32.30.Bv, 31.30.Jv

Rydberg states of helium have proven to be an excellent system for testing long-range physics in atoms. In Rydberg states, where one electron is found at large distances (typically $100a_0$ for $n = 10$) while the ion core is confined to shorter distance scales, measurements of fine-structure intervals test the long-range interactions between the electron and the core, including retardation (or Casimir) interactions. Precision tests of these interactions have been made possible in the past decade by increasing accurate theoretical calculations [1–3] of the structure of helium and high-precision measurements [4–8] of the Rydberg fine-structure intervals. We report here a 200 ppb measurement of the helium $n = 10$ $^+F_3$-$^+G_4$ interval, which is the most accurate measurement of any Rydberg fine structure. (Here the notation used is ^+L_J, where L is the orbital angular momentum, J is the total angular momentum, and the + indicates that the state is the higher energy of the two states that are mixtures of singlet and triplet.)

The measurement was done using separated-oscillatory-field (SOF) microwave-induced transitions (see Fig. 1). This method, first proposed by Ramsey [10] and later used to obtain high-precision measurements of the $n = 2$ Lamb shift in hydrogen [11], has the advantage of narrowing the resonant linewidth. The present measurement is the first application of the SOF technique to the precision study of Rydberg fine structure. A fast neutral beam of excited helium atoms is created by charge exchange between 4.00 (or 2.31) keV He^+ ions and a dense thermal beam of neutral cesium. Many of the helium ions neutralize into excited states, including the $n = 10$ states of interest. Those ions which do not neutralize are deflected out of the beam by a 8-kV/cm dc field, which also serves to Stark ionize and remove very high-n atoms. The population of $10F$ atoms is depleted by exciting $10F$ atoms up to the $27G$ state using a $^{12}C^{18}O_2$ laser tuned to the I $P(26)$ line, with the angle of intersection between the CO_2 laser beam and the atomic beam being used to Doppler tune the laser frequency. After passing through the microwave fields in which the 10 $^+G_4$-$^+F_3$ transition is driven, the beam passes through a second CO_2 laser beam, this one tuned to the $10G$-$27H$ resonance. The $27H$ atoms are then Stark ionized and deflected into a channeltron electron multiplier (CEM). The number of $27H$ states excited and thus the current seen on the CEM is decreased whenever atoms are driven from the 10 $^+G_4$ to the $^+F_3$ state in the microwave fields.

Two waveguides (WR430, $B1$ and $B2$ in Fig. 1) are directed perpendicular to the atomic beam and are used for the separated oscillatory fields. The microwaves are generated by a Anritsu model MG3602A signal generator which is stabilized to an accuracy of 10^{-11} using a Stellar model 100B satellite connection to the Global Positioning Satellite time base. A Narda model SS122DHS microwave SPDT switch driven at 221 Hz alternatively connects the signal generator to the E or H ports of a Struthers M352M waveguide magic tee (MT in Fig. 1). The connection is made by type-N cable which passes into the 1-m-diam vacuum chamber using Amphenol UG-300/U feedthroughs followed by Scientific Atlantic 11-1.7 type-N to WR430 waveguide adapters. The magic tee produces microwaves on the two output ports which are in phase when connected to the H input port, and 180° out of phase when connected to the E input port. The two output ports are connected via Struthers E13OM waveguide bends to $B1$ and $B2$ which are aimed downward and which have 0.400 × 0.800-in. rectangular holes to allow the atomic beam to pass through. $B1$ and $B2$ are separated by 38.620 in. (center to center).

Data were obtained using an EG&G 5105 square-wave lock-in amplifier which extracts the signal synchronous

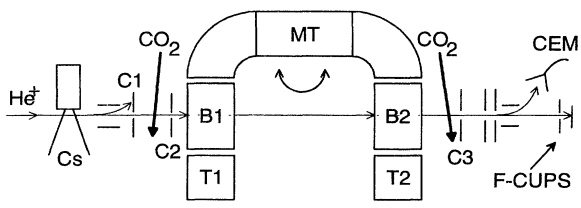

FIG. 1. A schematic of our experimental setup. Details are described in the text. Further details of some portions of the apparatus are given in Ref. [9].

with the switching from 0° to 180° relative phases. The CO_2 laser beams were chopped at 470 Hz (with a 90% on, 10% off duty cycle) and a second lock-in amplifier was used to record the signal synchronous with this chopping. This signal was used as a diagnostic and to normalize the main microwave signal.

The data were taken in 12 sets, with each set being taken on a separate 20-h day. Between each data set, the configuration of the microwave setup was changed (as described later) and the vacuum chamber re-evacuated to pressures of about 6×10^{-7} Torr.

To minimize the effects of Doppler shifts, we took the measurements with the microwaves and atomic beam as nearly perpendicularly as possible. In addition, we repeated the measurements with the direction of propagation of the microwaves reversed.

The position and direction of the atomic beam was determined by the three collimators shown in Fig. 1: $C1$, $C2$, and $C3$, which were separated by 28 and 122 cm and had heights of 0.041, 0.045, and 0.120 in., respectively. The beam current was monitored on a three-section Faraday cup at the end of the beam line. By adjusting the beam-focusing parameters in the source, it was possible to keep the relative sizes of the beams on each cup nearly constant throughout the measurements. $B1$ and $B2$ were placed perpendicular to the center of the collimators to an accuracy of 0.4 mrad. To allow for precision alignment of the waveguides and the precise reversal of the microwave propagation direction, $B1$ and $B2$ were precision machined (to tolerances of better than 0.001 in.) and very securely positioned within the vacuum chamber to be parallel and square to each other to within 0.001 in. $B1$ and $B2$ were left in position throughout the measurements. The magic-tee-elbow assembly was constructed with the output flanges of the elbows coplanar and square, so that they could be connected using dowel pins to either the top or the bottom of $B1$ and $B2$.

Another concern is the relative phase of the microwaves at the two points where they intersect the atomic beam. Any change from the nominal phases of 0° and 180° would cause significant shifts to the SOF line center. To deal with this concern, we took data with the magic-tee-elbow assembly (which was kept in one piece throughout the measurement) reversed as shown by the arrow in Fig. 1. The output ends of the main waveguide sections were connected (also with dowel pins) to precision Struthers model 200M waveguide terminators ($T1$ and $T2$ in Fig. 1), which were specified to have reflections of $|\Gamma| \leq 0.02$. The dowel pin connections assured that the waveguide and elbow assembly and the terminators could be removed and replaced while preserving their position to within 0.001 in. The positions of $B1$ and $B2$ were also checked to a precision of 0.001 in. before and after each data run using a high-power surveyor's scope.

The reversals described above made for a total of four configurations for the experimental setup. Three separate data sets were taken in each configuration. The average of data taken in the four configurations gives a result which is independent of first-order Doppler shifts and of microwave phase mismatches. Each data set consisted of data taken at two different beam speeds.

Line centers were obtained from fits such as those shown in Fig. 2. The expected line shape [11] is that of Ramsey SOF oscillations of $\cos(\Delta\omega T)$ within a Rabi envelope function which has a width of $1/\tau$. Here T is the time of flight for the atoms passing from the center of one waveguide to the center of the other, τ is the time the atoms spend in each of the waveguide sections, and $\Delta\omega = \omega_G - \omega_F - \omega$. In the configuration of the present experiment, $T = 2.94$ and 2.23 μs and $\tau = 0.164$ and 0.124 μs for the 2.31 and 4.00 keV beams, respectively. These can be compared to the lifetime of these states of $\tau_{10F} = 1.08$ μs and $\tau_{10G} = 1.81$ μs. The exact SOF line shape for two decaying states (in the rotating field approximation, assuming sudden turn on and off of the fields) can be obtained from Eq. (55) of Ref. [11]. To include the effects of the antirotating field, of the other states in the system, and of the fact that the microwave field ramps up slowly as the atoms enter the waveguide sections, we numerically integrated the Schrödinger equation (including all the relevant helium $n = 10$ states) [12] in the presence of the microwave fields. These calculations confirm that the expected shape is symmetric and nearly sinusoidal. The rate of the oscillations obtained from fits such as that of Fig. 2 is consistent with the beam speeds and powers used.

Shown in Table I are the average fit values for the centers in the various experimental configurations. The variation between different runs taken in the same configuration was somewhat larger than the statistical errors. We attribute this to the fact that the average direction of the atomic beam may have varied from run to run, by 0.4 mrad, which seems reasonable given the size of our collimators and the readings on our split Faraday cup.

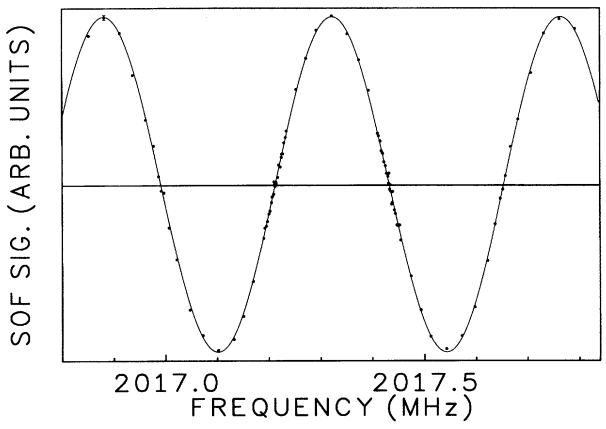

FIG. 2. Data taken at 4.00 keV. Note the excellent agreement with the expected line shape.

TABLE I. Systematic corrections and corrected line centers for the various experimental configurations. All values are given in kHz, with one standard deviation errors given in parentheses. BB denotes blackbody and Nbr. denotes neighboring.

Expt. configuration	Fit center	ac shift	dc shift	Time dil.	BB shift	Nbr. res.	Corrected centers
Magic T normal dir.	2 017 323.02(41)	0.12(3)	1.10(20)	1.73(2)	−0.17(2)	0.00(6)	2 017 325.80(46)
Magic T reversed dir.	2 017 322.95(39)	0.12(3)	1.14(20)	1.78(2)	−0.17(2)	0.00(6)	2 017 325.82(44)
Magic T on top	2 017 323.07(39)	0.12(3)	1.16(20)	1.75(2)	−0.17(2)	0.00(6)	2 017 325.93(44)
Magic T on bottom	2 017 322.89(40)	0.12(3)	1.09(20)	1.77(2)	−0.17(2)	0.00(6)	2 017 325.70(45)
2.309 keV beam	2 017 323.50(42)	0.09(2)	0.91(20)	1.25(1)	−0.17(2)	0.00(3)	2 017 325.58(47)
4.001 keV beam	2 017 322.56(38)	0.16(4)	1.29(20)	2.17(2)	−0.17(2)	0.00(9)	2 017 326.01(44)
Normal μwave power	2 017 323.28(36)	0.18(4)	1.08(20)	1.74(2)	−0.17(2)	0.00(9)	2 017 326.11(42)
Quarter μwave power	2 017 322.49(46)	0.04(1)	1.19(20)	1.79(2)	−0.17(2)	0.00(2)	2 017 325.34(50)
Average values	2 017 322.98(29)	0.12(3)	1.12(20)	1.76(2)	−0.17(2)	0.00(6)	2 017 325.8(4)

Since data were taken in both directions of microwave propagation, this variation of the beam position does not cause any systematic shift, but it does increase the size of our statistical errors. The difference of 0.1(6) kHz between the first two rows of the table indicates that there was very little phase mismatch between the two arms of the microwave system. The difference of 0.2(6) kHz between the third and fourth row indicates that the atomic beam was (on average) perpendicular to the microwave propagation direction to within 0.2 mrad. Also shown in the table are the averaged centers obtained at the two beam velocities and at the two microwave powers.

A number of systematic corrections are listed in Table I. The ac Stark shift (or power shift) can be calculated from

$$\Delta_{\mathrm{ac}\,i} = \sum (eE_{\mu\mathrm{wave}} z_{ik}/2)^2/(E_i - E_k \pm hf),$$

where the sum is over all states k and includes both the plus and minus signs. For the resonant term, only the plus sign is used, and this term is referred to as the Bloch-Siegert shift. Since the atoms spend most of their time in a field-free region between the two microwave regions, the ac Stark shift is reduced by approximately a factor of τ/T, and this approximation is sufficient for the small ac shifts in this measurement. The exact ac shift can be obtained from our numerical integration of the Schrödinger equation. The field-size $E_{\mu\mathrm{wave}}$ is estimated from the saturation behavior of the F-to-G resonance. The uncertainty in the ac shift is small and is due to the uncertainty in the distribution of m-level populations (each m has a different ac shift) and the uncertainty in $E_{\mu\mathrm{wave}}$.

The dc Stark shift is due to small stray fields of approximately 10 mV/cm rms which are present. Care was taken to reduce these fields by using similar metals to avoid contact potentials, by canceling the Earth's magnetic field (to $<$10 mG) in order to avoid motional electric fields, and by heating the waveguide assembly to 330 K to discourage dirty surfaces which would otherwise cause surface charging. The size of the field was measured by monitoring the position of the 20^3D_2-20^3F_3 resonance which occurs [13] at 1999.435 MHz in zero dc field. This resonance shifts at a rate of $-360(20)$ MHz/(V/cm)^2, which is much faster than the $-6.4(3)$ MHz/(V/cm)^2 shift rate of the $10F$-G resonance. The error estimates are due to the different shift rates of the different m levels. Throughout the data collection, the $20D$-F data scans were taken interspersed with the $10F$-G data. The $10F$-G centers are corrected for the dc Stark shifts by multiplying the shift in the $20D$-F resonance by the ratio of the shift rates.

The position of the 20^3D_2-20^3F_3 resonance is complicated by the presence of the nearby 20^3D_1-20^3F_2 and 20^3D_3-20^3F_4 resonances. This complication is minimized by the choice of 2.31 and 4.00 keV beams, since at these two speeds, the sinusoidal signals from the two neighboring peaks are in phase with the main resonance and thus cause very little shift in its center. The effect of the neighboring peaks has been modeled by full integration of the Schrödinger equation. The experimental shape of the resonances and the shift of the main resonance shows a dependence on microwave power which agrees with the calculations. The uncertainties in the dc Stark shifts listed in Table I include a 10 kHz uncertainty in the zero-dc-field position of the 20^3D_2-20^3F_3 resonance due to the presence of the nearby resonances.

Table I also shows the correction of $+\beta^2 f/2$ due to time dilation and the ac Stark shifts caused by the blackbody radiation present in the microwave regions which were on average at a temperature of 315 K. The latter can be calculated using the formalism of Farley and Wing [14]. The uncertainties in these corrections are small.

The ${}^+F_3$-${}^+G_4$ interval was chosen for this measurement because it is well resolved ($>$20 MHz) from the other F-G transitions, but neighboring $10F$-G resonances were modeled (using time-dependent perturbation theory and numerical integration of Schrödinger's equation) to give small shifts. The sign of the shifts is unknown because it depends too sensitively on the rate of oscillations of the SOF signals, and so we have included in Table I an uncertainty equal to the largest modeled shifts.

Several other systematic corrections were small and need not be included. The variation of microwave power with frequency (in each of the arms and when fed by each port of the magic tee) was $<$0.3% per MHz. This effect was modeled using the SOF line shape of Ref. [11], and found to cause a shift of less than 15 Hz. The balance of power in two microwave arms was found to be equal to

within 10% and causes no shift. A set of data was taken at 9 times higher pressure and, as expected, indicated no shift in frequency.

The final result for the interval is shown in Table I: 2017.3258(4) MHz. This compares poorly with a previous measurement of the interval [6] of 2017.3110(31) MHz. The reason for the discrepancy is unknown and a matter of some concern. However, we note that because of the perpendicular microwave propagation, the SOF configuration, our ability to vary the beam speed, and the large signal-to-noise ratio which allowed us to take data at a variety of parameters, our systematic uncertainties are smaller than in the previous measurement. Also, we note that the present measurement has a narrower resonant width and much better signal-to-noise ratio.

The best theoretical prediction for the interval comes [2] from the variational calculations of Drake who predicts 2017.3254(4) MHz, in good agreement with our measurement. This calculation does not, however, include certain long-range retardation (Casimir) corrections that have been calculated directly in a long-range QED calculation [3]. This correction of -0.0012 MHz (referred to as $V''_{\rm ret}$) shows the limitation of standard atomic physics calculations in calculating long-range interactions and represents the onset of the long-range behavior of the Casimir interaction. With this correction, the theoretical prediction is 2017.3242(4) MHz, which is 1.6 kHz below our measured value. The discrepancy is 4 times our experimental uncertainty and 2.7 times the combined theoretical and experimental uncertainties. Thus, our measurement indicates that the long-range Casimir interaction is not present. The only other measurement to date of long-range Casimir forces on microscopic systems is by Sukenik *et al.* [15], who measure the force between a sodium atom and two conducting planes. The results which they find in their very different systems, confirm the long-range Casimir interaction in that system. A second possible interpretation of our present results is that the long-range Casimir interaction is, in fact, present and that there are also significant additional interactions, indicating new long-range physics in these large-sized atoms. One example of such additional interactions could be a spin-dependent part of the long-range Casimir interaction, which has not yet been calculated. Either interpretation indicates a problem with the present understanding of long-range QED interactions.

The level of agreement between the present measurement and Drake's theory is consistent with the agreement (at 1 ppm) in the $n = 10$ D-F intervals [8] and in the $n = 5$ F-G interval (at 5 ppm) [7], but is in contrast to the 5 ppm discrepancies found at higher L [5]. This level of agreement confirms the total retardation contribution to this interval (0.1853 MHz) and the QED (one- and two-electron Lamb shift) contributions (0.0669 MHz) to an accuracy of better than 1%. The total relativistic contribution (10.5268 MHz) is tested to an accuracy of 0.004% and, of course, the nonrelativistic Coulomb interaction is tested at the 10^{-7} level of accuracy.

This work was supported by the Natural Sciences and Engineering Research Council of Canada.

[1] R. J. Drachman, Phys. Rev. A **47**, 694 (1993); C. K. Au, G. Feinberg, and J. Sucher, Phys. Rev. Lett. **53**, 1145 (1984); E. A. Hessels, Phys. Rev. A **46**, 5389 (1992); J. F. Babb and L. Spruch, Phys. Rev. A **38**, 13 (1988).

[2] G. W. F. Drake, in *Long Range Casimir Forces: Theory and Recent Experiments in Atomic Systems,* edited by F. S. Levin and D. Micha (Plenum, New York, 1993); G. W. F. Drake and Z. C. Yan, Phys. Rev. A **46**, 2378 (1992).

[3] C. K. Au and M. A. Mesa, Phys. Rev. A **41**, 2848 (1990).

[4] S. L. Palfrey and S. R. Lundeen, Phys. Rev. Lett. **53**, 1141 (1984); E. A. Hessels, W. G. Sturrus, and S. R. Lundeen, Phys. Rev. A **38**, 4574 (1988).

[5] E. A. Hessels, P. W. Arcuni, F. J. Deck, and S. R. Lundeen, Phys. Rev. A **46**, 2622 (1992).

[6] E. A. Hessels, F. J. Deck, P. W. Arcuni, and S. R. Lundeen, Phys. Rev. A **41**, 3663 (1990); **44**, 7855(E) (1991).

[7] Y. Kriescher, O. Hilt, and G. V. Oppen, Z. Phys. D **29**, 103 (1994).

[8] N. E. Claytor, E. A. Hessels, and S. R. Lundeen, Phys. Rev. A **52**, 165 (1995).

[9] N. E. Rothery, C. H. Storry, and E. A. Hessels, Phys. Rev. A **51**, 2919 (1995).

[10] N. F. Ramsey, *Molecular Beams* (Oxford University Press, London, 1956).

[11] S. R. Lundeen and F. M. Pipkin, Metrologia **22**, 9 (1986).

[12] Numerical integration to accuracies of 10 ppb took considerable computing power and was done using a band of 50 496 DX computers.

[13] G. W. F. Drake, Adv. At. Mol. Op. Phys. **32**, 93 (1993).

[14] J. W. Farley and W. H. Wing, Phys. Rev. A **23**, 2397 (1981).

[15] C. I. Sukenik, M. G. Boshier, D. Cho, V. Sandoghdar, and E. A. Hinds, Phys. Rev. Lett. **70**, 560 (1993).